

# Microfluidic velocimetry reveals spatial cooperativity in soft glassy flows

J. Goyon,<sup>1</sup> A. Colin,<sup>1,\*</sup> G. Ovarlez,<sup>2</sup> A. Ajdari,<sup>3</sup> L. Bocquet,<sup>4,5,\*</sup>

<sup>1</sup> LOF, Université Bordeaux 1, UMR CNRS-Rhodia-Bordeaux 1 5258,  
33608 Pessac cedex, France

<sup>2</sup> LMSGC, Université Paris Est, Institut Navier, 77420 Champs sur Marne, France

<sup>3</sup> UMR CNRS Gulliver 7083, ESPCI, 75005 Paris, France

<sup>4</sup> Laboratoire PMCN, Université Lyon 1; Université de Lyon,  
UMR CNRS 5586, 69622 Villeurbanne, France

<sup>5</sup> Physics Department, Technische Universität München, 85748 Garching, Germany

E-mail: lyderic.bocquet@univ-lyon1.fr, annie.colin-exterieur@eu.rhodia.com

(Dated: January 21, 2021)

**Amorphous glassy materials of diverse nature – concentrated emulsions, granular materials, pastes, molecular glasses – display complex flow properties, intermediate between solid and liquid, which are at the root of their use in many applications [1, 2, 3]. A classical feature, well documented yet not really understood, is the very non-linear nature of the flow rule relating stresses and strain rates [4, 5]. Using a microfluidic velocimetry technique, we characterize the flow of thin layers of concentrated emulsions, confined in gaps of different thicknesses by surfaces of different roughness. Beyond the classical non-linearities of the rheological behaviour, we evidence finite size effects in the flow behaviour and the absence of an intrinsic local flow rule. In contrast, a rather simple non-local flow rule is shown to account for all the velocity profiles. This non-locality of the dynamics is quantified by a length, characteristic of the cooperativity of the flow at these scales, that is unobservable in the liquid state (lower concentrations) and that increases with concentration in the jammed state. Beyond its practical importance for applications involving thin layers, e.g. coatings, our assessment of non-locality and cooperativity echoes observations on other glassy, jammed and granular systems, suggesting a possible fundamental universality.**

Glasses and jammed matter are at the heart of many challenging questions in condensed matter physics. The glass transition and the physical and mechanical properties of materials in the glassy or jammed state, from granular materials to dense colloidal suspensions, remain puzzle to a large extent [2, 3, 4, 5, 6, 7, 8]. The transition itself is characterized by a dramatic slowing down of the system, associated with a dynamical arrest of the microscopic structure [3]. While a large amount of work has been dedicated in recent years to demonstrating and characterizing dynamical heterogeneities in granular, glassy and glass forming materials [9, 10, 11, 12, 13, 14, 15, 16], the question of whether

and how these dynamical heterogeneities influence the flow behaviour remains [17, 18, 19]. Indeed one expects that such cooperative effects, which are in essence dynamical processes, should manifest themselves in the flow dynamics of jammed materials. This question is essential from the perspective of both fundamental science and applications: flows of jammed and glassy materials and glassy films are ubiquitous in nature and industry, *e.g.* in granular flows, coatings with thin polymer films, lubricating process in solid friction, in the food and cosmetic industries, and even in pedestrian dynamics [20].

In the present work, we aim to develop a constitutive law governing flows of jammed materials. We take advantage of a local velocity measurement technique to follow the local flow behaviour of a film of a confined soft glassy material (here a concentrated emulsion). We demonstrate the existence of *finite-size effects in the flow dynamics* that cannot be apprehended within our current understanding of the behaviour of yield stress fluids.

As schematized in Fig. 1, we probe the flow of a jammed emulsion in various geometries and confinements: shear or pressure driven planar flow; wide gap Couette cell (one centimeter gap) or narrow microchannel (from tens to hundreds of microns in width). The emulsion is made of silicone droplets ( $\approx 6.5\mu\text{m}$  in diameter) in an index-matched glycerine-water mixture (Supplementary Information, Method). We are specifically interested in the *local flow curves* of the material, which relate the local shear stress  $\sigma$  to the local shear rate  $\dot{\gamma}$ , Fig. 1C-D. Such curves can be constructed from the velocity profiles measured in the jammed emulsion in both geometries using local velocimetry techniques (Supplementary Information, Method), see insets of Fig. 1C-D. Indeed in both geometries the stress distribution is known from mechanical equilibrium:  $\sigma(R) = \frac{\Gamma}{2\pi HR^2}$  at a position  $R$  in the Couette cell (of height  $H$ ) under a torque  $\Gamma$ ;  $\sigma(z) = \frac{\Delta P}{L}(z - \frac{w}{2})$ , at a position  $z - \frac{w}{2}$  from the centerline of the microchannel, under an applied pressure drop  $\Delta P$  between the two ends of the channel of length  $L$  [21]. Local shear rates  $\dot{\gamma}$  are deduced directly from the velocity profiles. As shown in Figs. 1C and 1D, the local flow curves exhibit very different behaviours depending on the confinement of the material. In the *wide* gap Couette cell, all local flow curves obtained for different torques show

a perfect superposition (Fig 1.C). The flow curve is furthermore well described by a classical Herschel-Bulkley (HB) model,  $\sigma = \sigma_0 + A\dot{\gamma}^{1/2}$ , with  $\sigma_0$  a 'dynamical' yield stress and  $A$  a material constant. On the other hand, in the *narrow* microchannels, data for different pressure drops  $\Delta P$  are scattered in the whole figure and do not collapse on a single rheological curve (Fig 1.D), see also Supplementary Figure SI-4. Accordingly, while a single HB model accounts perfectly for all the velocity profiles in the wide gap Couette cell (inset of Fig.1.C), *such is not the case for the narrow microchannels* (Supplementary Figure SI-8). Furthermore, *below the jamming point*,  $\phi < \phi_c$ , the local HB rheological model is fully able to reproduce the flow behaviour, even in narrow channels (Supplementary Figure SI-3). In summary, a first key feature emerges from the experimental data: in the jammed state,  $\phi > \phi_c$ , *there is no universal local relationship between stress and shear rate*.

As a further confirmation of this point, the overall shape of the velocity profiles, for the same wall shear stress, is shown to vary with the thickness of the channel (Fig. 2), demonstrating *finite-size effects in the flow properties* of the jammed emulsion. Rougher surfaces are shown to induce higher shear rates for the same confinement and shear stress at the wall. We did furthermore verify that the above results do not stem from a structural change of the emulsion itself: we checked that neither the size distribution of the droplets, nor their shape, was affected by the flow and in all the geometries no variation of local droplet concentration was measured within the gap (Supplementary Method). Altogether, our results suggest that the flow does not couple to a structural order parameter, so that non-local effects are 'intrinsic' to the rheology of the jammed emulsion, in line with similar observations in numerical simulations for glassy flows [17].

A second crucial feature is the *experimental proof of a specific surface rheology* at the channel walls, distinct from the bulk flow behaviour. First, as commonly observed in flows of concentrated systems, slip effects show up at the confining walls [22]. We have characterized these effects by measuring the velocity slip-surface stress relationship (Fig. 3a), for two different roughness (Supplementary Method and Supplementary Figure SI-2). Strikingly, a remarkable collapse of the data is exhibited for various confinements and pressure drops, suggesting that this relationship does only depend on the surface roughness, see also Supplementary Figure SI-7a. However, a careful inspection of Fig. 2 shows that beyond slip effects, the *shape* itself of the flow profiles does depend on the surface characteristics of the confining wall, suggesting that the wall roughness makes the system more fluid. In an attempt to rationalize this behaviour we plot the wall shear rate as a function of the wall shear stress in Fig. 3b (see also Supplementary Figure SI-7b). Again a striking collapse of all data for various confinements and pressure drops is exhibited. We emphasize that such a behaviour is not expected *a priori* since the same wall

stress can be achieved with different confinements and pressure drops.

On the basis of these experimental facts, we now propose a theoretical framework able to rationalize these finite-size effects in the rheological behaviour. In concentrated emulsions, and more generally in soft glasses, flow occurs via a succession of reversible elastic deformations and local irreversible plastic rearrangements associated with a microscopic yield stress [23, 24, 25, 26]. These localized plastic events induce a non-local, long ranged, elastic relaxation of the stress over the system. The number of plastic rearrangements per unit time,  $\nu$ , plays the role of an inverse relaxation time and therefore controls the flow and relaxation of the material: a higher rate is associated with a more fluid system. Up to an elastic modulus  $G$ , the rate of rearrangements  $\nu$  is equivalent to a "fluidity",  $f$ , defined as  $\sigma = \frac{1}{f}\dot{\gamma}$ , a quantity that has been used in recent studies to characterize the rheology of yield stress fluids [25]. In the absence of any non-local effect, the fluidity would reduce to its *bulk* value,  $f_{\text{bulk}} = \dot{\gamma}/\sigma_{\text{bulk}}$  [note that for the HB expression reported above,  $f_{\text{bulk}} \propto \dot{\gamma}$  in the quasistatic limit, as  $\sigma \rightarrow \sigma_0$ ]. Now, due to the non-local elastic relaxation of plastic rearrangements ('dynamical cooperativity') [24, 26], a dynamically active region will induce agitation of its neighbours, and thus a higher rate of plastic rearrangements (and vice-versa for a dynamically quiescent region). This suggests that non-local effects will occur for the rearrangements rates and consequently for the fluidity,  $f$ . In order to capture this physical picture, we assume that the local fluidity,  $f(z)$ , obeys a non-local equation in the steady state:

$$f(z) = f_{\text{bulk}} + \xi^2 \frac{\partial^2 f(z)}{\partial z^2} \quad (1)$$

In this equation, the non-local term describes how the plastic activity spreads spatially over the system due to non-local elastic relaxation: it accounts for the cooperativity involved in the plastic events occurring during flow and  $\xi$  denotes a bulk 'flow cooperativity length'.

Together with the definition  $f(z) = \dot{\gamma}(z)/\sigma(z)$ , Eq. (1) constitutes our non-local rheological model for the emulsion. An analytical solution of Eq. (1) can be obtained, giving the fluidity at some position  $z$  in terms of an integral of the shear-stress over the whole channel width. For convenience we solved Eq. (1) numerically with  $f(z) = \dot{\gamma}_{\text{wall}}/\sigma_{\text{wall}}$  as a given boundary condition at the walls and  $f = 0$  in the centerline. Velocity profiles are deduced by integrating the computed local shear rate  $\dot{\gamma}(z)$ . Let us first note that whatever the boundary condition at the wall the solution of Eq. (1) can not reduce to its local form,  $f_{\text{bulk}}(z) = f_{\text{bulk}}(\sigma(z))$ , due to the diffusive, non-local term.

The only remaining parameter is the bulk 'flow cooperativity length'  $\xi$  in Eq. (1). A crucial and surprising finding is that *a unique (constant) length  $\xi$  accounts for all experimental data for the flow profiles and local flow curves for a given emulsion, Figs. 1.D and 2, inde-*

pendently of the pressure drop, confinement and surface nature (rough or smooth). That so much data can be fitted using a single and constant length  $\xi$  is quite remarkable. Typical comparisons are shown in Figs. 1D and 2 for both the velocity profiles and the corresponding local flow curves (see also Supplementary Figures SI-5, SI-6). We mention that alternative non-local rheological models, involving *e.g.* non-local terms in the flow curve [27] are unable to reproduce all measured flow profiles, Supplementary Figure SI-9.

Furthermore, a similar, very good agreement has been obtained for all (jammed) emulsions investigated, with various volume fractions and polydispersities (Supplementary Figures SI-5 and SI-6). Fig. 4 reports the variation of the measured flow cooperativity length  $\xi$  as a function of the volume fraction for emulsions with two different dispersities. Below the jamming concentration  $\phi < \phi_c$ , we could not measure finite-size effects in the flow profiles within the experimental uncertainty (Supplementary Figure SI-3), so that  $\xi \approx 0$  in this case. A strong increase of  $\xi$  is observed above the jamming threshold, in line with the appearance of elastic and yield properties of the materials in this regime.

Non-local effects in the flow properties may be *a priori* expected at the microscopic scale [27]. However, we measure a 'flow cooperativity length' only in the jammed state, providing a direct and novel connection between non-local effects and the jamming transition. Furthermore, we emphasize that this length is associated with correlations of a dynamical quantity (the fluidity, *i.e.* re-

arrangements) and not with static structural order. Typically for the volume fraction range studied here,  $\xi$  varies between 0 and 30 microns, to compare with the droplet size  $d \approx 6\mu\text{m}$ , giving roughly a cooperatively rearranging region involving up to a few hundreds of particles. These values are close to estimates for the dynamical heterogeneities measured in glassy materials [10, 11] or in jammed granular materials [14, 16, 28]. Furthermore, similar observations of non-locality have been reported in granular flows close to the jamming transition [15, 29], suggesting further universal characteristics.

However, we emphasize that the present length characterizing flow cooperativity differs fundamentally from that which characterizes dynamical heterogeneities involved in spontaneous fluctuations. Indeed, while these dynamical heterogeneities have been measured to exhibit a maximum at the jamming point [10, 30], the present flow cooperativity length  $\xi$  is non-vanishing in the jammed region only, and increases when going deeper in the jammed phase. This suggests that the flow behaviour of glassy and jammed materials involves physical mechanisms distinct from those associated with the glass transition. We expect that the flow cooperativity length  $\xi$  measures the zone of influence of localized plastic events occurring during flow and not the size of mobile regions. Our results thus provides a novel perspective for developing a theoretical framework to describe the non-local flow behaviour of glassy and jammed systems, such as soft glasses and granular materials.

- 
- [1] Jop, P., Y. Forterre, Y., Pouliquen, O., A constitutive law for dense granular flows, *Nature* **441**, 727 (2006).
  - [2] Debenedetti, P.G., Stillinger, F.H., Supercooled liquids and the glass transition *Nature* **410**, 259 (2001).
  - [3] Biroli, G., A new kind of phase transition ? *Nature Physics* **3**, 222 (2007).
  - [4] Coussot, P., Rheophysics of pastes: a review of microscopic modelling approaches, *Soft Matter* **3** 528 (2007).
  - [5] Fuchs, M., Cates, M.E., Theory of nonlinear rheology and yielding of dense colloidal suspensions, *Phys. Rev. Lett.* **89**, 248304 (2002).
  - [6] Goldenberg, C., Goldhirsch, I., Friction enhances elasticity in granular solids, *Nature* **435** 188-191 (2005)
  - [7] Ostojic, S., Somfai, E., Nienhuis, B., Scale invariance and universality of force networks in static granular matter *Nature* **439** 828-830 (2006)
  - [8] Liu, A.J., Nagel, S. R., Jamming is not just cool any more, *Nature* **396**, 21-22 (1998).
  - [9] Berthier, L., Time and length scales in supercooled liquids, *Phys. Rev. E* **69**, 020201(R) (2004).
  - [10] Weeks, E.R., Crocker, J.C., Levitt, A.C., Schofield, A., Weitz, D.A., Three dimensional direct imaging of structural relaxation near the colloidal glass transition, *Science* **287**, 627-631 (2000).
  - [11] Berthier L., Biroli, G., Bouchaud, J.-P., Cipelletti, L., Masri, D. El., L'Hôte, D., Ladieu, F., Pierno, M., Direct experimental evidence of a growing length scale accompanying the glass transition, *Science* **310**, 1797-1800 (2005).
  - [12] Gao, Y., Kilfoil, M.L., Direct imaging of dynamical heterogeneities near the colloid-gel transition, *Phys. Rev. Lett.* **99**, 078301 (2007).
  - [13] Priestley, R.D., Ellison, C.L., Broadbelt, L.J., Torkelson, J.M., Structural relaxation of polymer glasses at surfaces, interfaces and in between *Science* **309**, 456-459 (2005)
  - [14] Dauchot, O., Marty, G., Biroli, G., Dynamical Heterogeneity close to the Jamming transition in a sheared granular material, *Phys. Rev. Lett.* **95**, 265701 (2005).
  - [15] Pouliquen, O., Velocity Correlations in dense granular flows, *Phys. Rev. Lett.* **93**, 248001 (2004).
  - [16] Keys, A. S., Abate, A. R., Glotzer, S.C., Durian, D. J., Measurement of growing dynamical length scales and prediction of the jamming transition in a granular material, *Nature Physics* **3**, 260-264 (2007).
  - [17] Varnik, F., Bocquet, L., Barrat, J.-L., Berthier, L., Shear localization in a model glass, *Phys. Rev. Lett.* **90**, 095702 (2003).
  - [18] Leonforte, F., Tanguy, A., Wittmer, J.P., Barrat, J.-L., Inhomogeneous elastic response of Silica glass, *Phys. Rev. Lett.* **97**, 055501 (2006).
  - [19] Isa, L., Besseling, R., Poon, W.C., Shear Zones and Wall Slip in the Capillary Flow of Concentrated Colloidal Suspensions, *Phys. Rev. Lett.* **98**, 198305 (2007).
  - [20] Helbing, D., Farkas, I., Vicsek, T., Simulating dynamical

- features of escape panic, *Nature* **407**, 487-490 (2000).
- [21] Degré, G., Joseph, P., Tabeling, P., Lerouge, S., Cloitre, M., Ajdari, A. Rheology of complex fluids by particle image velocimetry in microchannels *Appl.Phys.Lett.* **89**, 024104 (2006).
- [22] Meeker, S.P., Bonnecaze, R.T., Cloitre, M., Slip and Flow in Soft Particle Pastes, *Phys. Rev. Lett.* **92** 198302 (2004).
- [23] Princen, H. M., Rheology of foams and highly concentrated emulsions, *J. Colloid Interface Sci.* **91**, 160-175 (1983).
- [24] Schall, P., Weitz, D.A., Spaepen, F., Structural rearrangements that govern flow in colloidal glasses, *Science* **318**, 1895 (2007).
- [25] Picard, G., Ajdari, A., Bocquet, L., Lequeux, F., A simple model for heterogeneous flows of yield stress fluids, *Phys. Rev. E* **66**, 051501 (2002).
- [26] Picard, G., Ajdari, A., Lequeux, F., Bocquet, L., Slow flows of yield stress fluids : complex spatiotemporal behavior within a simple elastoplastic model, *Phys. Rev. E* **71**, 010501(R) (2005).
- [27] Dhont, J. K. G., A constitutive relation describing the shear-banding transition *Phys. Rev. E* **60**, 4534-4544 (1999).
- [28] Kamrin, K., Bazant, M.Z., A stochastic flow rule for granular materials *Phys. Rev. E* **75**, 041301 (2007).
- [29] Deboeuf, S., Lajeunesse, E., Dauchot, O., Andreotti, B., Flow rule, Self-channelization and levees in unconfined granular flows, *Phys. Rev. Lett.* **97**, 158303 (2006).
- [30] Goldman, D.I., Swinney, H.L., Signatures of glass formation in a fluidized bed of hard spheres, *Phys. Rev. Lett.* **96** 145702 (2006).

**Acknowledgements:** Discussions with Jean-Louis Barrat and Bruno Andreotti are gratefully acknowledged. This project was supported by Rhodia, Région Aquitaine and the ANR. L.B. acknowledges support from the von Humboldt foundation.

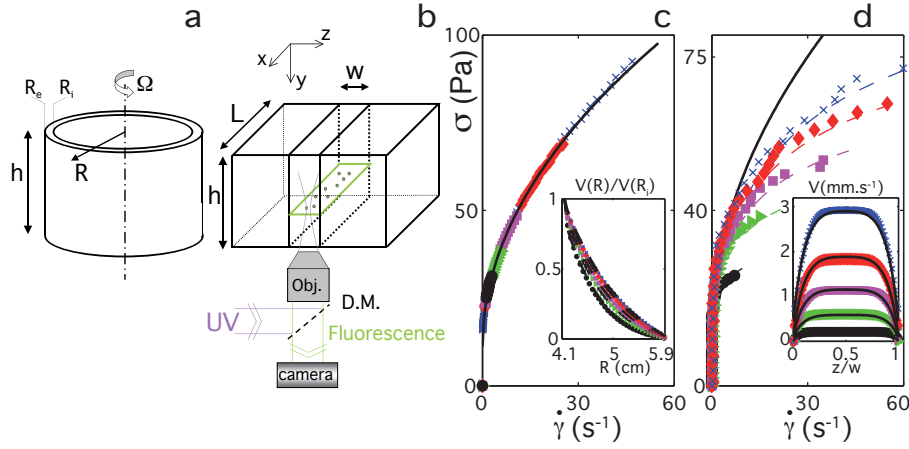


FIG. 1: **Local flow curves measured by IRM and Microfluidic velocimetry.**

*Left:* Schematic of the experimental set up. (A) wide gap Couette cell (inner and outer cylinder radii,  $R_i = 4.1\text{cm}$ , and  $R_e = 5.9\text{cm}$  respectively, height  $h = 11\text{cm}$ ). (B) Flow in a microchannel and particle imaging velocimetry. PIV : (DM): Dichroic mirror; UV : Ultra-Violet lamp; Obj : microscope objective. Flow direction is along  $x$ . *Right:* Local flow curves extracted from the measurements of the velocity profiles in both geometries for an emulsion with volume fraction  $\phi = 0.75$  and 20% polydispersity. The shear rates are obtained by finite differencing of the velocity profiles given in the insets. (C) Local flow curves,  $\sigma(z)$  versus  $\dot{\gamma}(z)$ , extracted from the velocity profiles measured within a wide gap Couette geometry (see inset). The solid line corresponds to the Herschel-Bulkley model with  $\sigma_0 = 11.6 \text{ Pa}$ ,  $A = 11.2 \text{ Pa}\cdot\text{s}^{1/2}$ . *Inset:* Dimensionless velocity profiles  $\frac{V(R)}{V(R_i)}$  as a function of the radial coordinate  $R$ . From bottom to top the rotation velocity is 5, 10, 20, 50 and 100 rpm. (D) Local flow curves,  $\sigma(z)$  versus  $\dot{\gamma}(z)$ , extracted from the velocity profiles measured in a  $w = 250\mu\text{m}$  thick microchannel with rough surfaces, for various pressure drops as a function of the reduced coordinate  $z/w$  (see inset). No overlap of the local flow curves is observed. Dashed lines are predictions for the local flow curves at the given  $\Delta P$ , as obtained from the non-local rheological model of Eq. (1) with a cooperativity length  $\xi = 22.3\mu\text{m}$ . The solid line corresponds to the Herschel-Bulkley model with  $\sigma_0 = 11.6 \text{ Pa}$ ,  $A = 11.2 \text{ Pa}\cdot\text{s}^{1/2}$ . *Inset:* Corresponding velocity profiles measured for  $\Delta P$  equal to 300, 450, 600, 750, 900 mbar. The length of the channel is  $L = 14 \text{ cm}$ . Solid lines are the velocity profiles predicted by the non-local rheological model of Eq. (1). Slippage, which is found to occur at the surfaces as detailed in Fig. 3, does not affect the resulting local flow curves as plotted in the main figure.

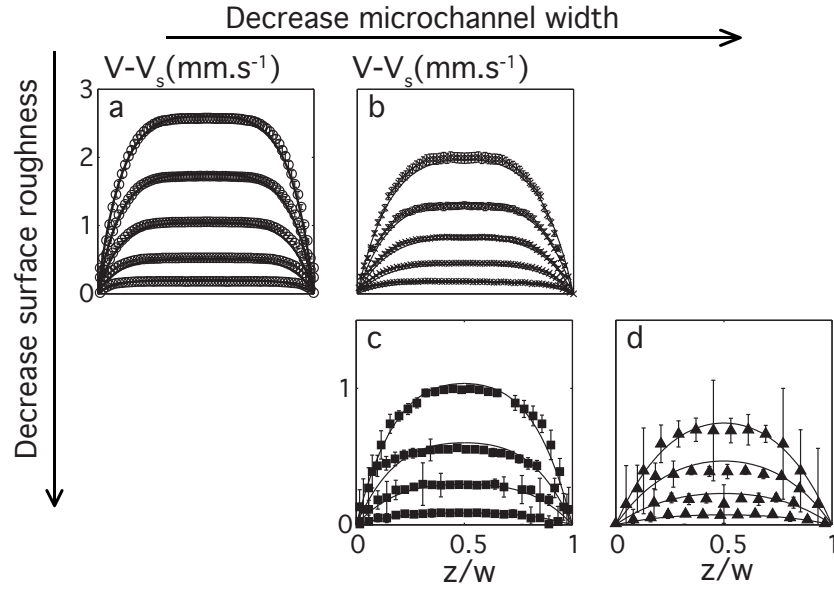


FIG. 2: **Velocity profiles in microchannels with different gaps  $w$  and confining wall roughness, corrected for the slip velocity:** (a)  $\circ$  rough microchannel with  $w = 250 \mu\text{m}$ ; (b)  $\times$  rough microchannel with  $w = 125 \mu\text{m}$ , (c)  $\blacksquare$  smooth microchannel with  $w = 112 \mu\text{m}$ ; (d)  $\blacktriangle$  smooth microchannel with  $w = 56 \mu\text{m}$ . Solid lines are velocity profiles predicted by the non local model of Eq. (1) with a length  $\xi = 22.3\mu\text{m}$ . The various experimental velocity profiles correspond to different pressure drops  $\Delta P$ , tuned to get the same range of wall shear stress  $\sigma_{\text{wall}}$  in the various geometries. From bottom to top the values of  $\sigma_{\text{wall}}$  are: (a) 27, 41, 55, 68, 82 Pa; (b) 30, 45, 60, 75, 90 Pa; (c) 45, 60, 75, 91 Pa; (d) 48, 65, 82, 97 Pa. The volume fraction is  $\phi = 75\%$ , with 20% polydispersity. Errobars denote s.d. ( $n=450$ ).

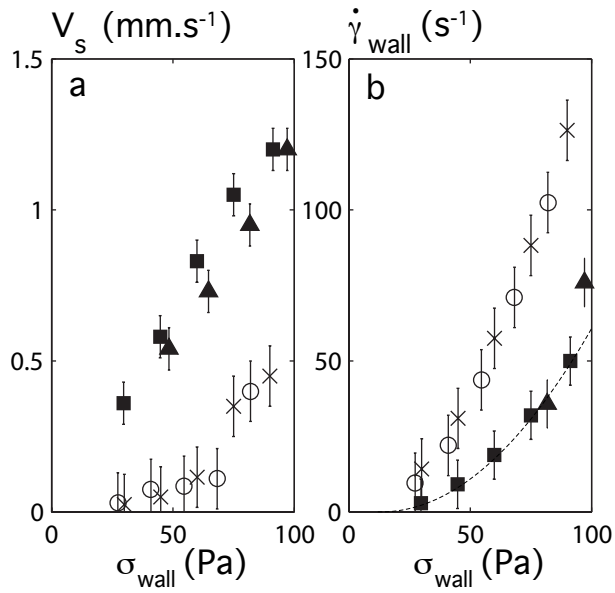


FIG. 3: **Rheology at surfaces:** (a) Slip velocity at the wall as a function of the wall shear stress for various microchannels; (b) Shear rate at the confining wall  $\dot{\gamma}_{\text{wall}}$  as a function of the wall shear stress  $\sigma_{\text{wall}}$  for various microchannels. The dashed line is the bulk flow curve (Herschel-Bulkley model with  $\sigma_0 = 11.6 \text{ Pa}$ ,  $A = 11.2 \text{ Pa}\cdot\text{s}^{1/2}$ ). Data gather different pressure drops  $\Delta P$  and confinements  $w$ . Symbols are identical to those in Figure 2. Open (filled) symbols correspond to rough (smooth) confining surfaces. The volume fraction is  $\phi = 75\%$ , with 20% polydispersity. Errobars on the velocity denote s.d. ( $n=450$ ).

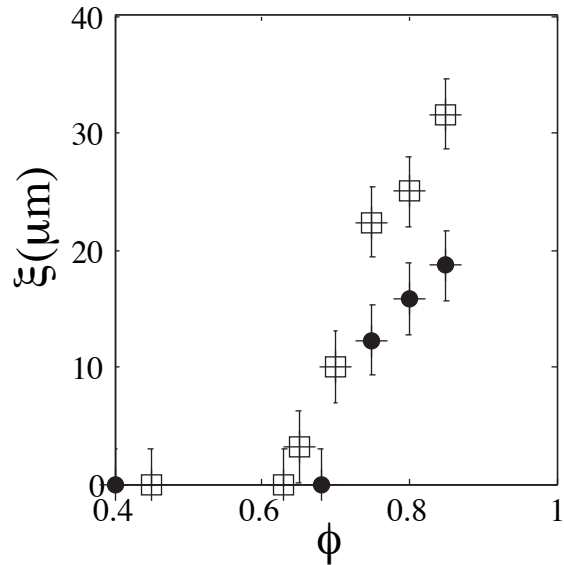


FIG. 4: **Flow cooperativity length  $\xi$  as a function of emulsion volume fraction.** Open and filled symbols corresponds to emulsions with different polydispersities of 20% (open) and 36% (filled) respectively. The corresponding jamming volume fraction, as determined by the occurrence of a non-vanishing yield stress, are  $\phi_c = 0.64$  (open) and  $\phi_c = 0.68$  (filled). Errorbars denote the dispersion of the experimental values over various experiments.